Interaction of particles in a deformed nematic liquid crystal

Jun-ichi Fukuda,[1] Bohdan I. Lev,[1,2] Keiko M. Aoki,[1] and Hiroshi Yokoyama[1,3]
[1]*Yokoyama Nano-structured Liquid Crystal Project, ERATO, Japan Science and Technology Corporation, 5-9-9 Tokodai, Tsukuba 300-2635, Japan*
[2]*Department of Theoretical Physics, Institute of Physics, NAS Ukraine, Prospekt Nauki 46, Kyiv 04022, Ukraine*
[3]*Nanotechnology Research Institute, AIST, 1-1-4 Umezono, Tsukuba 305-8568, Japan*
(Received 22 September 2001; revised manuscript received 26 August 2002; published 21 November 2002)

We investigate how the interaction of particles mediated by an elastic deformation of a nematic liquid crystal is influenced by the initial deformation of the director field. To this end, we calculate the interaction energy between particles in a nematic cell with hybrid boundary conditions, homeotropic on the surface of one confining plate and planar on the other. We find an analytic form of the interaction energy in the case of weak anchoring on the surface of the particle. This interaction energy sensitively depends on the position of the two particles as well as the interparticle distance and can be nonmonotonic with a minimum in its landscape. This nontrivial energy landscape might lead to a chainlike superstructure of particles.

DOI: 10.1103/PhysRevE.66.051711 PACS number(s): 61.30.Cz, 82.70.Dd

I. INTRODUCTION

Colloidal systems and emulsions have attracted a great deal of interest in technology because of their various practical applications [1,2]. They have also become an important subject of fundamental science and it is of much interest how the constituent particles or droplets in such systems interact with each other and what kinds of structures and phases these interactions will bring about. The colloidal interactions mediated by the host fluid include van der Waals, electrostatic, depletion [1,3], and fluctuation-induced [4] and surface-induced [5,6] forces.

Recently, growing attention has been paid to colloidal suspensions and emulsions with anisotropic host fluids like liquid crystals as a class of composite materials [7–12]. One of the characteristic feature of liquid crystal emulsions and colloids is that the liquid crystals surrounding the particles are deformed because of anchoring on the surfaces of the particles. When the anchoring is strong enough, the particles are accompanied by topological defects such as a hyperbolic hedgehog [8,13], a Saturn ring [14,15], or boojums [13]. Theoretical [16–19] and numerical [20–24] studies have been devoted to understanding the formation of topological defects.

Another interesting and important property of liquid crystal emulsions and colloids is that the particles can interact via the elastic deformation of liquid crystals due to the surface anchoring of the particles, which can be directly measured experimentally [25]. This elasticity-mediated interaction, which is of course absent in the usual colloidal suspensions and emulsions with an isotropic host fluid, has proved to play a crucial role in yielding a wide variety of superstructures that have not been observed in conventional colloidal systems. One of the striking examples experimentally observed is a linear-chain superstructure [8,13,26,27], and anisotropic clusters [7,14] and periodic lattices [28] have also been reported. The investigation and evaluation of the elasticity-mediated interaction is therefore quite significant for understanding and predicting the essential properties and behaviors of superstructures in liquid crystal colloids and emulsions. There have been several theoretical studies, and as early as 1978 Lopatnikov and Namiot [29] made an analytic calculation of the interaction U between cylindrical particles in a nematic liquid crystal to obtain an anisotropic long-range form of dipole-dipole type with $U \sim r^{-3}$, where r is the interparticle distance. Later, Ramaswamy *et al.* [30] and Ruhwandl and Terentjev [31] found a quadrupole interaction $U \sim r^{-5}$ in the case of spherical particles in a nematic liquid crystal with weak surface anchoring. A quadrupole interaction is known to be responsible for the formation of a chain of particles with boojum defects [13,27] and the direction of the chain is oblique to the orientation of the host nematic liquid crystal. Lubensky *et al.* showed by a phenomenological argument that a linear-chain structure [8,13,26] parallel to that of the host nematic liquid crystal can be attributed to the interaction between ''dipoles'' composed of a particle and an accompanying hedgehog defect. The interaction between the ''dipoles'' was investigated also by a numerical computation [32]. We note that similar theoretical attempts have also been made on the particle interaction in a smectic liquid crystal due to the layer displacement [29,33,34]. It should also be pointed out that the recent theoretical and experimental progress has stimulated numerical studies on the aggregation process and structure formation in liquid crystal colloids [35,36].

Recently, one of the present authors (B.I.L.) developed a theoretical scheme for calculating the interaction potential in a nematic liquid crystal [37]. It is similar to previous theories [29–31] in that the elastic deformation is assumed to be weak enough to evaluate the director field as an expansion in terms of the deformation from the ground state. This assumption facilitates an analytic treatment of the problem. One of the main advantages of the treatment of Ref. [37] over the previous ones is that it can be applied to general cases of particles with arbitrary shape and anchoring orientation on the surface by introducing tensors characterizing the geometry of the particles. It has been shown [37,38] that the symmetry of the particles crucially influences the properties of the interaction between them. In the case of spherical particles the interaction is of quadrupolar nature like $U \sim r^{-5}$ as

noted above, while for less symmetric particles dipolar interactions $U \sim r^{-3}$ or even Coulomb interactions $U \sim r^{-1}$ can be expected. Moreover, we do not have to restrict the initial state of the nematic liquid crystal to be uniform, and in a recent paper [39] we considered the interaction potential in a cholesteric liquid crystal using this framework.

In this paper, utilizing the latter advantage we discuss how the particle interaction is influenced by the initial deformation of the host liquid crystal. This work is motivated by a recent experiment [28] showing the formation of a two-dimensional crystal structure by glycerol droplets dispersed in a nematic liquid crystal. In this experiment the host nematic is deformed due to the boundary conditions. At the upper boundary the liquid crystal interfaces with the air, which leads to a homeotropic orientation there. On the other hand, a tangential boundary condition is imposed on the lower boundary with glycerol, that is, liquid crystal molecules tend to align parallel to this boundary. So far as we know, this is the only experimental study of an emulsion in a deformed liquid crystal [40], and no theoretical studies have been devoted to the effect of the initial deformation of a liquid crystal on the interaction between particles immersed in it. Confining a liquid crystal by boundaries with different anchoring implies the introduction of a length scale (note that the Frank elasticity of a nematic liquid crystal [41] has no characteristic lengths) together with a nonuniform structure. We can therefore expect richer and less trivial properties than in the case of a uniform nematic liquid crystal. Although our theoretical setup is slightly different from that in the experiment of Ref. [28] in that the liquid crystal orientation at the lower boundary is fixed in our calculation, we believe that our theoretical investigation will shed light on the possible effect of the initial deformation of liquid crystals on the structure of liquid crystal colloids.

This article is organized as follows. In Sec. II we give a detailed theoretical procedure to obtain an analytic form of the interaction potential. Using this result we discuss how particles interact in a deformed nematic liquid crystal in Sec. III. We conclude this article in Sec. IV together with a comparison of our theoretical results with the experimental findings.

II. CALCULATION OF THE INTERACTION POTENTIAL

A. Formulation of the problem

We consider a nematic liquid crystal confined between two parallel plates with the distance d as depicted in Fig. 1. We set the z axis perpendicular to the plates and we set the origin so that the two plates are located at $z=0$ and d. We impose strong homeotropic and planar boundary conditions at $z=d$ and 0, respectively, with the in-plane orientation fixed along the x axis at $z=0$. This geometrical setup is similar to that in the experiment by Nazarenko *et al.* [28] and different in that the molecular orientation at the lower boundary has a fixed in-plane orientation in our treatment. We impose the fixed boundary condition here for the simplicity of the calculation. In the case of the one-constant approximation in the Frank elastic energy, it is easy to show that the ground state of the director field is

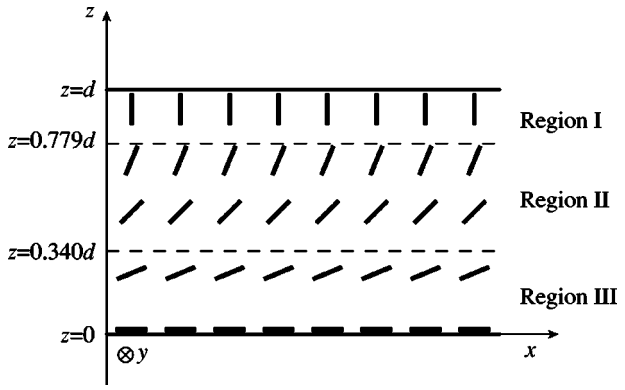

FIG. 1. Illustration of the geometry of our system. The definition of regions I, II, and III is given in Sec. III A.

$$\boldsymbol{n}^{(0)}(z) = (\cos q_0 z, 0, \sin q_0 z), \tag{1}$$

with

$$q_0 \equiv \frac{\pi}{2d}, \tag{2}$$

which indeed satisfies the boundary conditions and the equilibrium condition $\nabla^2 \boldsymbol{n} \| \boldsymbol{n}$ [41].

To describe the deformation of the director field with respect to the ground state, we introduce the deformation fields $u(\boldsymbol{r})$ and $v(\boldsymbol{r})$ and the director field $\boldsymbol{n}(\boldsymbol{r})$ can be written as

$$\boldsymbol{n}(\boldsymbol{r}) = (\cos[q_0 z + u(\boldsymbol{r})]\cos v(\boldsymbol{r}), \sin v(\boldsymbol{r}), \sin[q_0 z + u(\boldsymbol{r})]\cos v(\boldsymbol{r})). \tag{3}$$

Notice that $u(\boldsymbol{r}) = v(\boldsymbol{r}) = 0$ at $z=0$ and d because we deal with the situation where the boundary conditions are strong enough.

The bulk Frank elastic energy in the one-constant approximation can be written as [42]

$$F_b = \frac{1}{2} K \int d^2 \boldsymbol{r}_\perp (\partial_i n_j)(\partial_i n_j), \tag{4}$$

with K being the elastic constant and $\boldsymbol{r}_\perp = (x,y)$. Here $i,j = x$, y, or z and in this subsection summations over repeated indices are implied (except for x, y, and z below). We substitute Eq. (3) into Eq. (4) to describe the elastic energy in terms of the deformation fields u and v. Throughout this argument we restrict ourselves to the case of small deformations and we retain up to second order terms in u and v as in our previous study [37,39]. After some calculations, utilizing the property $u(\boldsymbol{r}) = v(\boldsymbol{r}) = 0$ at $z=0$ and d and assuming that the deformation vanishes at infinity, we arrive at

$$F_b = \frac{1}{2} K \int d^2 \boldsymbol{r}_\perp \int_0^d dz \{(\boldsymbol{\nabla} u)^2 + (\boldsymbol{\nabla} v)^2 - q_0^2 v^2\}. \tag{5}$$

Apparently this energy is not positive definite because it becomes smaller with increasing v as long as v is independent of the position ($\boldsymbol{\nabla} v = \boldsymbol{0}$). The deformation mode v corresponds to the rotation of the director out of the xz plane.

After rotating the director out of the xz plane by the angle $\pi/2$, the director becomes uniform (parallel to the y axis) and obviously the elastic energy is smaller than in the case of Eq. (1), which is the implication of the apparent breakdown of the positive definiteness of Eq. (5). In our case, however, such a rotation is prohibited because of the boundary conditions and the energy (5) is indeed positive definite. To show that and make the following discussion clear, we introduce the Fourier transform, taking the boundary conditions at $z=0$ and d into account, as

$$u(\boldsymbol{q}_\perp, q_z) = \int d^2\boldsymbol{r}_\perp \int_0^d dz e^{-i\boldsymbol{q}_\perp \cdot \boldsymbol{r}_\perp} \sin q_z z \, u(\boldsymbol{r}), \tag{6}$$

where $q_z = 2mq_0 = m\pi/d$, with m being a positive integer. We also define $v(\boldsymbol{q}_\perp, q_z)$ in the same way. By substituting the inverse Fourier transform

$$u(\boldsymbol{r}) = \frac{1}{(2\pi)^2} \int d^2\boldsymbol{q}_\perp \cdot \frac{2}{d} \sum_{m=1}^{\infty} e^{i\boldsymbol{q}_\perp \cdot \boldsymbol{r}_\perp} \sin 2mq_0 z \, u(\boldsymbol{q}_\perp, 2mq_0), \tag{7}$$

and the same form of $v(\boldsymbol{r})$ into Eq. (5), we obtain

$$\begin{aligned} F_b = \frac{1}{2} K \frac{1}{(2\pi)^2} \int d^2\boldsymbol{q}_\perp \cdot \frac{2}{d} \sum_{m=1}^{\infty} \{ & [\boldsymbol{q}_\perp^2 + (2mq_0)^2] \\ & \times u(\boldsymbol{q}_\perp, 2mq_0) u(-\boldsymbol{q}_\perp, 2mq_0) \\ & + [\boldsymbol{q}_\perp^2 + (4m^2-1)q_0^2] v(\boldsymbol{q}_\perp, 2mq_0) v(-\boldsymbol{q}_\perp, 2mq_0) \}, \end{aligned} \tag{8}$$

which is obviously positive definite. We notice here that the form of the elastic energy (8) will be sensitive to the boundary conditions. For instance, if a tangential boundary condition is imposed at $z=0$ so that the director can rotate freely on the $z=0$ plane, the allowed wave number in the z direction q_z will be different, which leads to a different expression of the free energy in reciprocal space [note that the free energy in real space (5) is unaltered for this boundary condition].

Next we consider how particles introduced in our system deform the director field. We write the surface energy on the particles in the Rapini-Papoular form [43] as

$$F_s = \sum_p \oint_{\Omega_p} d^2S W(\boldsymbol{s}) [\boldsymbol{\nu}(\boldsymbol{s}) \cdot \boldsymbol{n}(\boldsymbol{s})]^2. \tag{9}$$

Here p is the index labeling the particles and the surface of the particle p is denoted by Ω_p. The integral is taken over Ω_p and d^2S is the surface element. The anchoring strength is given by $W(\boldsymbol{s})$ and $\boldsymbol{\nu}(\boldsymbol{s})$ is the unit normal to the surface at the point $\boldsymbol{s}$. In the case of homeotropic anchoring, $W(\boldsymbol{s}) < 0$, and vice versa for planar anchoring.

We restrict ourselves to the case of weak anchoring ($|W| r_0/K \ll 1$, where r_0 is the characteristic dimension of the particles) so that the director field is only slightly deformed by the particles from its ground state [Eq. (1)] [44]. Then we can safely assume that the director field $\boldsymbol{n}(\boldsymbol{r})$ is defined throughout the system, even within particles, and continuous so that the Fourier transform (6) is well defined.

In dealing with the surface energy, we make a gradient expansion of the director field $\boldsymbol{n}(\boldsymbol{s})$ around the center of gravity of the particle p, which we will denote by $\boldsymbol{r}^{(p)}$. This treatment is justified when r_0 is sufficiently smaller than the characteristic length of the elastic distortion in a nematic liquid crystal (d in our case). Since the bulk energy F_b [Eqs. (4) and (5)] contains only terms up to second order in the gradients, it is sufficient to make a gradient expansion up to second order also for the surface energy F_s. Then the director field can be represented as

$$\begin{aligned} \boldsymbol{n}(\boldsymbol{s}) = \boldsymbol{n}(\boldsymbol{r}^{(p)}) + (\boldsymbol{s} - \boldsymbol{r}^{(p)})_i \frac{\partial}{\partial r_i^{(p)}} \boldsymbol{n}(\boldsymbol{r}^{(p)}) \\ + \frac{1}{2} (\boldsymbol{s} - \boldsymbol{r}^{(p)})_i (\boldsymbol{s} - \boldsymbol{r}^{(p)})_j \frac{\partial}{\partial r_i^{(p)}} \frac{\partial}{\partial r_j^{(p)}} \boldsymbol{n}(\boldsymbol{r}^{(p)}) + \cdots. \end{aligned} \tag{10}$$

We can formally write the director field as $\boldsymbol{n} = \boldsymbol{n}^{(0)} + \delta\boldsymbol{n}$, with $\boldsymbol{n}^{(0)}$ being the initial director field in the absence of particles defined in Eq. (1). After some calculations using Eq. (10), we find

$$\begin{aligned} [\boldsymbol{\nu}(\boldsymbol{s}) \cdot \boldsymbol{n}(\boldsymbol{s})]^2 \simeq \mathcal{A}_{kl}^{(p)} \Bigg(& \frac{1}{2} n_k^{(0)}(\boldsymbol{r}^{(p)}) n_l^{(0)}(\boldsymbol{r}^{(p)}) \\ & + n_k^{(0)}(\boldsymbol{r}^{(p)}) \delta n_l(\boldsymbol{r}^{(p)}) \Bigg) \end{aligned} \tag{11}$$

for the pth particle. Here we have defined the operator

$$\mathcal{A}_{kl}^{(p)} = \alpha_{kl}^{(p)} + \beta_{jkl}^{(p)} \frac{\partial}{\partial r_j^{(p)}} + \gamma_{ijkl}^{(p)} \frac{\partial}{\partial r_i^{(p)}} \frac{\partial}{\partial r_j^{(p)}}, \tag{12}$$

with $\alpha_{kl}^{(p)}$, $\beta_{jkl}^{(p)}$, and $\gamma_{ijkl}^{(p)}$ being tensors characterizing the geometry of the particles, defined as [37]

$$\alpha_{kl}^{(p)} = 2 \oint_{\Omega_p} d^2S W(\boldsymbol{s}) \nu_k(\boldsymbol{s}) \nu_l(\boldsymbol{s}), \tag{13}$$

$$\beta_{jkl}^{(p)} = 2 \oint_{\Omega_p} d^2S W(\boldsymbol{s}) (\boldsymbol{s} - \boldsymbol{r}^{(p)})_j \nu_k(\boldsymbol{s}) \nu_l(\boldsymbol{s}), \tag{14}$$

$$\gamma_{ijkl}^{(p)} = \oint_{\Omega_p} d^2S W(\boldsymbol{s})(\boldsymbol{s}-\boldsymbol{r}^{(p)})_i(\boldsymbol{s}-\boldsymbol{r}^{(p)})_j \nu_k(\boldsymbol{s})\nu_l(\boldsymbol{s}). \tag{15}$$

We note that in Eq. (11) we have retained only terms up to second order in the gradients as mentioned above and up to first order in $\delta\boldsymbol{n}$ as in the previous study [37]. Second order terms in $\delta\boldsymbol{n}$ will be required to discuss the effect of screening by particles on the interaction potential [38], which is beyond the scope of this work.

Noticing that $\delta\boldsymbol{n}(\boldsymbol{r}^{(p)}) \simeq (-u(\boldsymbol{r}^{(p)})\sin q_0 r_z^{(p)}, v(\boldsymbol{r}^{(p)}), u(\boldsymbol{r}^{(p)})\cos q_0 r_z^{(p)})$ [from Eq. (3)] and using Eq. (1), we obtain the resultant form of the surface energy as

$$\begin{aligned} F_s = & \frac{1}{2}\sum_p \mathcal{A}_{kl}^{(p)}[n_k^{(0)}(\boldsymbol{r}^{(p)})n_l^{(0)}(\boldsymbol{r}^{(p)})] \\ & + \sum_p \left\{ \frac{1}{2}(\mathcal{A}_{zz}^{(p)} - \mathcal{A}_{xx}^{(p)})[u(\boldsymbol{r}^{(p)})\sin 2q_0 r_z^{(p)}] \right. \\ & + \mathcal{A}_{xz}^{(p)}[u(\boldsymbol{r}^{(p)})\cos 2q_0 r_z^{(p)}] + \mathcal{A}_{xy}^{(p)}[v(\boldsymbol{r}^{(p)})\cos q_0 r_z^{(p)}] \\ & \left. + \mathcal{A}_{yz}^{(p)}[v(\boldsymbol{r}^{(p)})\sin q_0 r_z^{(p)}] \right\}. \end{aligned} \tag{16}$$

B. Energy of one particle

Before proceeding to the calculation of the interaction between particles mediated by the elastic deformation of the director field, we discuss here the energy of one particle arising from the interaction between a liquid crystal and the particle surface. First let us consider the contribution from the first order terms in W. The first term of Eq. (16) corresponds to it and from Eq. (1) it can be expressed as

$$\begin{aligned} & F_{s0}^{(p)}(\boldsymbol{r}^{(p)}) \\ & = \frac{1}{2}\left(\alpha_{xx}^{(p)} + \beta_{zxx}^{(p)}\frac{\partial}{\partial r_z^{(p)}} + \gamma_{zzxx}^{(p)}\frac{\partial^2}{\partial (r_z^{(p)})^2} \right)\cos^2 q_0 r_z^{(p)} \\ & \quad + \frac{1}{2}\left(\alpha_{zz}^{(p)} + \beta_{zzz}^{(p)}\frac{\partial}{\partial r_z^{(p)}} + \gamma_{zzzz}^{(p)}\frac{\partial^2}{\partial (r_z^{(p)})^2} \right)\sin^2 q_0 r_z^{(p)} \\ & \quad + \left(\alpha_{xz}^{(p)} + \beta_{zxz}^{(p)}\frac{\partial}{\partial r_z^{(p)}} + \gamma_{zzxz}^{(p)}\frac{\partial^2}{\partial (r_z^{(p)})^2} \right) \\ & \quad \times \cos q_0 r_z^{(p)} \sin q_0 r_z^{(p)}. \end{aligned} \tag{17}$$

Therefore, if the particle is highly symmetric so that

$$\begin{aligned} & \alpha_{xx}^{(p)} = \alpha_{zz}^{(p)}, \quad \beta_{zxx}^{(p)} = \beta_{zzz}^{(p)}, \quad \gamma_{zzxx}^{(p)} = \gamma_{zzzz}^{(p)}, \\ & \alpha_{xz}^{(p)} = \beta_{zxz}^{(p)} = \gamma_{zzxz}^{(p)} = 0, \end{aligned} \tag{18}$$

then $F_{s0}^{(p)}$ is independent of the particle position $\boldsymbol{r}^{(p)}$. Simple examples of a particle satisfying Eq. (18) are a spherical particle and a cylindrical particle whose axis is parallel to the y axis. In this case, to discuss the energetics of one particle, we have to take into account the contribution from the elastic deformation by the particles in liquid crystals, which is second order in W. It can be termed the self-energy and will be discussed briefly in the next subsection.

When Eq. (18) is not satisfied, $F_{s0}^{(p)}$ is a nonuniform function of $\boldsymbol{r}^{(p)}$, which implies that the particle is attracted or repelled by the boundaries depending on the precise form of the geometry tensors $\alpha_{kl}^{(p)}$, $\beta_{jkl}^{(p)}$, and $\gamma_{ijkl}^{(p)}$. For instance, we consider a cylindrical particle with planar anchoring ($W>0$), whose axis is parallel to the x axis and the radius is $a \ll d$. When the contribution of the ends of the cylinder can be neglected, $\alpha_{zz}^{(p)} > \alpha_{xx}^{(p)} \simeq 0$, $\gamma_{zzzz}^{(p)} > \gamma_{zzxx}^{(p)} \simeq 0$, and $\alpha_{xz}^{(p)} = \beta_{ijk}^{(p)} = \gamma_{zzxz}^{(p)} = 0$, which leads to

$$F_{s0}^{(p)} \simeq \left(\frac{1}{2}\alpha_{zz}^{(p)} - 2q_0^2 \gamma_{zzzz}^{(p)} \right)\sin^2 q_0 r_z^{(p)} + \text{const.} \tag{19}$$

It is not difficult to show that $\gamma_{zzzz}^{(p)}/\alpha_{zz}^{(p)} \simeq 3a^2/8$; thus the first term in the parentheses of Eq. (19) dominates because $q_0^2 a^2 \sim (a/d)^2 \ll 1$. Noticing that $\alpha_{zz}^{(p)} > 0$, we can conclude that the energy of this cylinder is lower when $r_z^{(p)}$ is smaller, i.e., close to the lower plate. This is consistent with the intuitive argument that a cylinder with planar anchoring prefers its orientation along the director of the surrounding nematic liquid crystal. We also notice that the contribution from the self-energy cannot be neglected when the particle is sufficiently close to one of the boundaries that the elastic deformation of the liquid crystal is strong.

C. Interaction energy

Now we proceed to the calculation of the elasticity-mediated interaction energy. The total energy of the system F is the sum of the bulk energy F_b [Eq. (5)] and the surface energy [Eq. (16)]. We will denote the distortion profile that minimizes the total energy in the presence of particles by $(u_{\min}(\boldsymbol{q}_\perp, q_z), v_{\min}(\boldsymbol{q}_\perp, q_z))$, which can be determined through the conditions

$$\left.\frac{\delta(F_b+F_s)}{\delta u(\boldsymbol{q}_\perp, q_z)}\right|_{u_{\min}, v_{\min}} = \left.\frac{\delta(F_b+F_s)}{\delta v(\boldsymbol{q}_\perp, q_z)}\right|_{u_{\min}, v_{\min}} = 0. \tag{20}$$

We find from calculation of Eq. (20) that the resultant distortion can be represented as a superposition of those due to one particle, that is, $u_{\min}(\boldsymbol{q}_\perp, q_z) = \Sigma_p u_{\min}^{(p)}$ and $v_{\min}(\boldsymbol{q}_\perp, q_z) = \Sigma_p v_{\min}^{(p)}$. Here $u_{\min}^{(p)}$ and $v_{\min}^{(p)}$ are the distortions due to a single particle p and written as

$$u_{\min}^{(p)}=u_{\min}^{(p)}(\boldsymbol{q}_\perp,q_z=2mq_0,\boldsymbol{r}^{(p)})$$
$$=-\frac{1}{K[\boldsymbol{q}_\perp^2+(2mq_0)^2]}\mathcal{D}_1^{(p)}\sin 2mq_0r_z^{(p)}\times\exp(-i\boldsymbol{q}_\perp\cdot\boldsymbol{r}_\perp^{(p)}), \quad (21)$$

$$v_{\min}^{(p)}=v_{\min}^{(p)}(\boldsymbol{q}_\perp,q_z=2mq_0,\boldsymbol{r}^{(p)})$$
$$=-\frac{1}{K[\boldsymbol{q}_\perp^2+(4m^2-1)q_0^2]}\mathcal{D}_2^{(p)}\sin 2mq_0r_z^{(p)}\times\exp(-i\boldsymbol{q}_\perp\cdot\boldsymbol{r}_\perp^{(p)}), \quad (22)$$

where we have defined the operators

$$\mathcal{D}_1^{(p)}g(\boldsymbol{r}^{(p)})=\frac{1}{2}(\mathcal{A}_{zz}^{(p)}-\mathcal{A}_{xx}^{(p)})[g(\boldsymbol{r}^{(p)})\sin 2q_0r_z^{(p)}]+\mathcal{A}_{xz}^{(p)}[g(\boldsymbol{r}^{(p)})\cos 2q_0r_z^{(p)}], \quad (23)$$

$$\mathcal{D}_2^{(p)}g(\boldsymbol{r}^{(p)})=\mathcal{A}_{xy}^{(p)}[g(\boldsymbol{r}^{(p)})\cos q_0r_z^{(p)}]+\mathcal{A}_{yz}^{(p)}[g(\boldsymbol{r}^{(p)})\sin q_0r_z^{(p)}], \quad (24)$$

with g being an arbitrary function.

The total energy can be obtained by substituting $u_{\min}(\boldsymbol{q}_\perp,q_z)$ and $v_{\min}(\boldsymbol{q}_\perp,q_z)$ into $F=F_b+F_s$, and the result is written as

$$F=\sum_p F_{s0}^{(p)}-\frac{K}{2}\frac{1}{(2\pi)^2}\int d^2\boldsymbol{q}_\perp\cdot\frac{2}{d}\sum_{m=1}^{\infty}\sum_p\sum_{p'}\{[\boldsymbol{q}_\perp^2+(2mq_0)^2]u_{\min}^{(p)}(\boldsymbol{q}_\perp,2mq_0,\boldsymbol{r}^{(p)})u_{\min}^{(p')}(-\boldsymbol{q}_\perp,2mq_0,\boldsymbol{r}^{(p')})$$
$$+[\boldsymbol{q}_\perp^2+(4m^2-1)q_0^2]v_{\min}^{(p)}(\boldsymbol{q}_\perp,2mq_0,\boldsymbol{r}^{(p)})v_{\min}^{(p')}(-\boldsymbol{q}_\perp,2mq_0,\boldsymbol{r}^{(p')})\}, \quad (25)$$

where $F_{s0}^{(p)}$ is the energy due to the anchoring on the surface of the particle and is given in Eq. (17). It can be further rewritten as $F=\Sigma_pF_1^{(p)}+\Sigma_{p<p'}U_{pp'}$ with $F_1^{(p)}$ and U_{pp} being the energy of one particle p and the pairwise interaction energy between particles p and p', respectively. The former is given by

$$F_1^{(p)}(\boldsymbol{r}^{(p)})=F_{s0}^{(p)}(\boldsymbol{r}^{(p)})-\frac{K}{2}\frac{1}{(2\pi)^2}\int d^2\boldsymbol{q}_\perp\cdot\frac{2}{d}\sum_{m=1}^{\infty}\{[\boldsymbol{q}_\perp^2+(2mq_0)^2]u_{\min}^{(p)}(\boldsymbol{q}_\perp,2mq_0,\boldsymbol{r}^{(p)})u_{\min}^{(p)}(-\boldsymbol{q}_\perp,2mq_0,\boldsymbol{r}^{(p)})$$
$$+[\boldsymbol{q}_\perp^2+(4m^2-1)q_0^2]v_{\min}^{(p)}(\boldsymbol{q}_\perp,2mq_0,\boldsymbol{r}^{(p)})v_{\min}^{(p)}(-\boldsymbol{q}_\perp,2mq_0,\boldsymbol{r}^{(p)})\}. \quad (26)$$

The second term of Eq. (26) is the self-energy due to the elastic deformation of the director field. Using Eqs. (21) and (22) and taking into account the double count in the summation $\Sigma_p\Sigma_{p'}$, we can write the interaction energy $U_{pp'}$ as

$$U_{pp'}(\boldsymbol{r}^{(p)},\boldsymbol{r}^{(p')})=-\frac{1}{K}\frac{1}{(2\pi)^2}\int d^2\boldsymbol{q}_\perp\cdot\frac{2}{d}\sum_{m=1}^{\infty}\left[\frac{1}{\boldsymbol{q}_\perp^2+(2mq_0)^2}\mathcal{D}_1^{(p)}\mathcal{D}_1^{(p')}+\frac{1}{\boldsymbol{q}_\perp^2+(4m^2-1)q_0^2}\mathcal{D}_2^{(p)}\mathcal{D}_2^{(p')}\right]$$
$$\times\sin 2mq_0r_z^{(p)}\sin 2mq_0r_z^{(p')}\exp[-i\boldsymbol{q}_\perp\cdot(\boldsymbol{r}_\perp^{(p)}-\boldsymbol{r}_\perp^{(p')})]. \quad (27)$$

After some calculations presented in the Appendix, we obtain

$$U_{pp'}(\boldsymbol{r}^{(p)},\boldsymbol{r}^{(p')})=-\frac{1}{4\pi K}\{\mathcal{D}_1^{(p)}\mathcal{D}_1^{(p')}[h_1(|\boldsymbol{r}_\perp^{(pp')}|,r_z^{(p)}-r_z^{(p')})-h_1(|\boldsymbol{r}_\perp^{(pp')}|,r_z^{(p)}+r_z^{(p')})]$$
$$+\mathcal{D}_2^{(p)}\mathcal{D}_2^{(p')}[h_2(|\boldsymbol{r}_\perp^{(pp')}|,r_z^{(p)}-r_z^{(p')})-h_2(|\boldsymbol{r}_\perp^{(pp')}|,r_z^{(p)}+r_z^{(p')})]\}, \quad (28)$$

where $\boldsymbol{r}_\perp^{(pp')}=\boldsymbol{r}_\perp^{(p)}-\boldsymbol{r}_\perp^{(p')}$ and

$$h_1(\xi,\eta)=\frac{1}{\sqrt{\xi^2+\eta^2}}+\sum_{m=1}^{\infty}\left\{\frac{1}{\sqrt{\xi^2+(\eta-2md)^2}}+\frac{1}{\sqrt{\xi^2+(\eta+2md)^2}}-\frac{1}{md}\right\}, \quad (29)$$

$$h_2(\xi,\eta)=\frac{\cos(q_0\sqrt{\xi^2+\eta^2})}{\sqrt{\xi^2+\eta^2}}+\sum_{m=1}^{\infty}\left\{\frac{\cos[q_0\sqrt{\xi^2+(\eta-2md)^2}]}{\sqrt{\xi^2+(\eta-2md)^2}}+\frac{\cos[q_0\sqrt{\xi^2+(\eta+2md)^2}]}{\sqrt{\xi^2+(\eta+2md)^2}}\right\}. \quad (30)$$

We note that $h_2(\xi,\eta)$ is associated with the variable v and its oscillating nature may be attributed to the presence of a negative contribution $-q_0^2 v^2$ in the free energy (5). This negative contribution reflects the fact that the initial deformed state is not a ground state and stabilized by the imposed boundary conditions as argued above. Although of course we cannot draw a general conclusion from this specific example, this kind of oscillation in the interaction potential might be a universal property in a deformed liquid crystal.

The self-energy, the second term of Eq. (26), is formally written as $(1/2)U_{pp'}(\boldsymbol{r}^{(p)},\boldsymbol{r}^{(p')})|_{\boldsymbol{r}^{(p)}=\boldsymbol{r}^{(p')}}$ and is regarded as the energy of the elasticity-mediated interaction between the particle and the confining surfaces. Evidently, however, it is not well defined due to the singular terms in Eqs. (29) and (30). Unfortunately, these singularities cannot be safely removed because they depend on $r_z^{(p)}$ through the operators $\mathcal{D}_{1,2}^{(p)}$. To discuss the self-energy properly, one must go back to Eq. (26) and introduce some cutoff in both the integral with respect to $\boldsymbol{q}_\perp$ and the summation with respect to m.

In a uniform nematic, the equations determining the equilibrium distortion profile [the same as Eq. (20)] are Poisson equations [37] and we can utilize the analogy with electrostatics. Then the interaction between a particle and a surface is equal to that between the particle and its image with the same sign and is always repulsive. In the case of a spherical particle this interaction energy can be explicitly written, apart from a numerical factor, as $U\sim(Wr_0^4)^2/KR^5$, with r_0 and R being the particle radius and the distance between the particle and the wall, respectively [see also Eq. (37) below]. As in Sec. III A below, we can expect that the result above for a uniform nematic can be applied to our case of a deformed nematic when R is sufficiently smaller than d, the distance between the confining surfaces. The equilibrium distance between a particle and a surface is determined by the balance between this elastic force and others such as gravity, buoyancy, and the van der Waals force [28].

III. DISCUSSION

Since the resultant form of the interaction energy (28) is still complicated, we restrict the discussion below to several specific cases. Moreover, we consider only the simple case of spherical particles with equal radius r_0. Then a straightforward calculation yields

$$\frac{1}{2}(\mathcal{A}_{zz}^{(p)}-\mathcal{A}_{xx}^{(p)})=\Gamma[(\partial_z^{(p)})^2-(\partial_x^{(p)})^2], \tag{31}$$

$$\mathcal{A}_{ij}^{(p)}=2\Gamma\partial_i^{(p)}\partial_j^{(p)} \quad (i\neq j), \tag{32}$$

with $\Gamma\equiv 4\pi W r_0^4/15$ and $\partial_j^{(p)}\equiv\partial/\partial r_j^{(p)}$, which leads to

$$\mathcal{D}_1^{(p)}g(\boldsymbol{r}^{(p)})=\Gamma\{\sin 2q_0 r_z^{(p)}[(\partial_z^{(p)})^2-(\partial_x^{(p)}+2q_0)^2] + 2\cos 2q_0 r_z^{(p)}(\partial_x^{(p)}+2q_0)\partial_z^{(p)}\}g(\boldsymbol{r}^{(p)}), \tag{33}$$

$$\mathcal{D}_2^{(p)}g(\boldsymbol{r}^{(p)})=2\Gamma\{\cos q_0 r_z^{(p)}(\partial_x^{(p)}+q_0) + \sin q_0 r_z^{(p)}\partial_z^{(p)}\}\partial_y^{(p)}g(\boldsymbol{r}^{(p)}). \tag{34}$$

A. The case with $|\boldsymbol{r}^{(p)}-\boldsymbol{r}^{(p')}|\to 0$

When we are interested in the limiting case with $|\boldsymbol{r}^{(p)}-\boldsymbol{r}^{(p')}|\to 0$ (to be more precise, $|\boldsymbol{r}^{(p)}-\boldsymbol{r}^{(p')}|\ll d$), we have to retain only the singular contributions in Eq. (28). Noticing that the summations in Eqs. (29) and (30) remain finite for $x,y\to 0$, we have

$$U_{pp'}\simeq-\frac{1}{4\pi K}\left[\mathcal{D}_1^{(p)}\mathcal{D}_1^{(p')}\frac{1}{r^{(pp')}}+\mathcal{D}_2^{(p)}\mathcal{D}_2^{(p')}\frac{\cos q_0 r^{(pp')}}{r^{(pp')}}\right], \tag{35}$$

where $r^{(pp')}=|\boldsymbol{r}^{(pp')}|\equiv|\boldsymbol{r}^{(p)}-\boldsymbol{r}^{(p')}|$ is the distance between particles p and p'. Since in this case $q_0\ll\partial_i^{(p)}\sim 1/r^{(pp')}$ and $\partial_i^{(p)}f(\boldsymbol{r}^{(pp')})=-\partial_i^{(p')}f(\boldsymbol{r}^{(pp')})$ with f being an arbitrary function, the operators $\mathcal{D}_1^{(p)}$ and $\mathcal{D}_2^{(p)}$ can be greatly simplified to yield

$$U_{pp'}\simeq-\frac{\Gamma^2}{\pi K}\left(\boldsymbol{n}\cdot\frac{\partial}{\partial\boldsymbol{r}^{(p)}}\right)^2\left(\boldsymbol{n}\times\frac{\partial}{\partial\boldsymbol{r}^{(p)}}\right)^2\frac{1}{r^{(pp')}}, \tag{36}$$

where $\boldsymbol{n}\equiv\boldsymbol{n}^{(0)}[(\boldsymbol{r}^{(p)}+\boldsymbol{r}^{(p')})/2]$ is the director of the ground state [Eq. (1)] at $\boldsymbol{r}=(\boldsymbol{r}^{(p)}+\boldsymbol{r}^{(p')})/2$. After a straightforward calculation of Eq. (36), we obtain

$$U_{pp'}\simeq\frac{3\Gamma^2}{\pi K(r^{(pp')})^9}[8(\boldsymbol{n}\cdot\boldsymbol{r}^{(pp')})^4-24(\boldsymbol{n}\cdot\boldsymbol{r}^{(pp')})^2 \times(\boldsymbol{n}\times\boldsymbol{r}^{(pp')})^2+3(\boldsymbol{n}\times\boldsymbol{r}^{(pp')})^4]. \tag{37}$$

From Eq. (37) it can be shown that when we set $\cos\theta=(\boldsymbol{n}\cdot\boldsymbol{r}^{(pp')})/r^{(pp')}$, the interaction is attractive when $(30+4\sqrt{30})/70<\cos^2\theta<(30+4\sqrt{30})/70$ $(30.56°<|\theta|<70.12°$ or $109.88°<|\theta|<149.44°)$ and repulsive otherwise.

It is important to note that Eq. (37) is equivalent to the form of the interaction between spherical particles introduced in a nematic liquid crystal uniformly aligned along the $\boldsymbol{n}$ direction [37]. This result is quite natural because the nematic liquid crystal close to the particles is indeed oriented locally along the $\boldsymbol{n}$ direction. However, when we consider the usual experimental conditions [28], we encounter situations with $|\boldsymbol{r}_\perp^{(pp')}|\gtrsim r_z^{(p)}$ when the particles lie close to the lower confining plate and $|\boldsymbol{r}_\perp^{(pp')}|\gtrsim d-r_z^{(p)}$ when the particles are near the upper plate. Then the terms dropped in the above discussion cannot be safely neglected because $h_1(|\boldsymbol{r}_\perp^{(pp')}|,r_z^{(p)}+r_z^{(p')})$ has a singular term like $1/\sqrt{|\boldsymbol{r}_\perp^{(pp')}|^2+(r_z^{(p)}+r_z^{(p')})^2}$ in the former case and $1/\sqrt{|\boldsymbol{r}_\perp^{(pp')}|^2+(2d-r_z^{(p)}-r_z^{(p')})^2}$ in the latter [a similar argument holds also for $h_2(|\boldsymbol{r}_\perp^{(pp')}|,r_z^{(p)}+r_z^{(p')})$]. A full analysis of the interaction energy requires numerical calculations and it will be given in a following subsection.

B. The case with $|\boldsymbol{r}^{(p)}-\boldsymbol{r}^{(p')}|\to\infty$

In discussing the asymptotic behaviors for $|\boldsymbol{r}^{(p)}-\boldsymbol{r}^{(p')}|\to\infty$, it will be convenient to get back to the form of Eq. (A2) together with Eqs. (A3) and (A4) in the Appendix. Since the modified Bessel function $K_0(x)$ decays fast to behave as $K_0(x)\sim e^{-x}\sqrt{\pi/2x}$ for $x\to\infty$, only the first terms ($m=1$) in Eqs. (A3) and (A4) will be relevant and the resultant form of the interaction energy is

$$\begin{aligned}U_{pp'}\simeq&-\frac{1}{2\pi Kd}(\mathcal{D}_1^{(p)}\mathcal{D}_1^{(p')}K_0(2q_0|\boldsymbol{r}_\perp^{(pp')}|)\\&\times\{\cos[2q_0(r_z^{(p)}-r_z^{(p')})]-\cos[2q_0(r_z^{(p)}+r_z^{(p')})]\}\\&+\mathcal{D}_2^{(p)}\mathcal{D}_2^{(p')}K_0(\sqrt{3}q_0|\boldsymbol{r}_\perp^{(pp')}|)\\&\times\{\cos[2q_0(r_z^{(p)}-r_z^{(p')})]-\cos[2q_0(r_z^{(p)}+r_z^{(p')})]\}).\end{aligned}\tag{38}$$

Here we do not give a detailed discussion of the form of Eq. (38) but simply notice the absence of long-range interaction in our system, which is definitely attributed to the forbidding of the fluctuation of Goldstone type due to the boundary conditions as argued in Sec. II A.

C. Numerical analysis for $r_z^{(p)}=r_z^{(p')}$

As noted in Sec. III A, further analytical treatment of the resultant energy $U_{pp'}$ is unfortunately almost impossible because Eq. (28) contains unsolvable infinite series as well as fourth-order derivatives. Moreover, the interaction energy is dependent on four independent variables $(\boldsymbol{r}^{(pp')})_{x,y}$, $r_z^{(p)}$, and $r_z^{(p')}$. Therefore it is unrealistic to discuss the behavior of the interaction energy $U_{pp'}$ in this four-dimensional space. Here we consider the situation where the two particles lie in a plane parallel to the confining plates so that $r_z^{(p)}=r_z^{(p')}$, which can be realized more easily in experiments.

We first note that the numerical results presented below have been obtained with the aid of MAPLE 6.01. We also notice that in the numerical evaluations the infinite series $\Sigma_{m=1}^{\infty}$ have been replaced by summations of the first 200 terms $\Sigma_{m=1}^{200}$ and we observed almost no difference from the results obtained by taking the summations of the first 100 terms. Therefore the contribution to the summation from terms with $m>100$ can be safely neglected in the arguments below.

Before presenting the numerical results, we discuss the asymptotic behavior of the interaction energy at $r^{(pp')}\to 0$ using the result of Sec. III A. In our case where $r_z^{(p)}=r_z^{(p')}$, we can write the interparticle distance as $\boldsymbol{r}^{(pp')}=(r\cos\phi, r\sin\phi, 0)$ (hereafter we abbreviate $r^{(pp')}$ as r) and $\cos\theta=(\boldsymbol{n}\cdot\boldsymbol{r}^{(pp')})/r=\cos\phi\cos(q_0r_z^{(p)})$. Then if $\cos^2(q_0r_z^{(p)})<(30-4\sqrt{30})/70$, i.e., $r_z^{(p)}>0.779d$, $\cos^2\theta<(30-4\sqrt{30})/70$ is always satisfied and the interaction is repulsive at $r^{(pp')}\to 0$ for all ϕ. We will denote this region $r_z^{(p)}>0.779d$ as region I. On the other hand, when $(30-4\sqrt{30})/70<\cos^2(q_0r_z^{(p)})<(30+4\sqrt{30})/70$, that is, $0.340d<r_z^{(p)}<0.779d$, we can determine the angle ϕ_1 that satisfies

$$\cos^2(q_0r_z^{(p)})\cos^2\phi_1=\frac{30-4\sqrt{30}}{70},\tag{39}$$

and at $r^{(pp')}\to 0$ the interaction is attractive when $|\cos\phi|>|\cos\phi_1|$ and repulsive otherwise. The region $0.340d<r_z^{(p)}<0.779d$ will be denoted as region II below. Finally, when $\cos^2(q_0r_z^{(p)})>(30+4\sqrt{30})/70$, i.e., $r_z^{(p)}<0.340d$, we can define ϕ_2 so that

$$\cos^2(q_0r_z^{(p)})\cos^2\phi_2=\frac{30+4\sqrt{30}}{70},\tag{40}$$

and at $r^{(pp')}\to 0$ the interaction is attractive when $|\cos\phi_1|<|\cos\phi|<|\cos\phi_2|$ and repulsive otherwise. This region will be denoted as region III.

In Fig. 2 we plot the reduced interaction energy $\bar{U}_{pp'}\equiv 4\pi Kd^5U_{pp'}/\Gamma^2$ as a function of the interparticle distance r for fixed ϕ in the case of $r_z^{(p)}=r_z^{(p')}=0.9d$ and $0.8d$, that is, the particles are in region I and close to the upper confining plate with homeotropic anchoring. Different curves in Fig. 2 correspond to different ϕ. We find from Fig. 2 that $\bar{U}_{pp'}$ has its minimum for ϕ smaller than some threshold value ($\simeq 15°$ and $30°$ for $r_z^{(p)}=0.9d$ and $0.8d$, respectively) and purely repulsive otherwise. For $r\to 0$, the interaction is repulsive for all cases as argued above. When the interaction potential has its minimum, the minimum position r becomes smaller and the absolute value of the minimum energy becomes larger for smaller ϕ and $r_z^{(p)}$. We also observe from the inset of Fig. 2(b) that a small maximum can also be present in the interaction potential and this oscillating nature may be attributed to the form of Eq. (30), containing trigonometric functions as mentioned in the previous section.

To observe the interaction energy landscape more clearly, we show contour plots of $\bar{U}_{pp'}$ in Fig. 3. Because of symmetry, mirror planes are present in these contour plots and it is therefore sufficient to show only the region $r_x^{(pp')}, r_y^{(pp')}>0$. It is obvious from Fig. 3 that $\bar{U}_{pp'}$ has its minimum at some finite $r_x^{(pp')}$ with $r_y^{(pp')}=0$. This implies that two particles tend to align parallel to the x axis (the direction of the fixed planar anchoring on one boundary) while keeping some finite distance. We also observe that the energy landscape is more deformed for $r_z^{(p)}$ $(=r_z^{(p')})=0.8d$, which is consistent with the oscillatory potential curve in the inset of Fig. 2(b).

We emphasize that such a potential minimum as obtained here has never been observed in the previous theoretical studies concerning the interaction between particles mediated by the elastic deformation of nematic liquid crystals. Then, other mechanisms such as the hard-core (or soft-core) repulsion, which are irrelevant in liquid crystals, must be incorporated to discuss the formation of superstructures of particles in a liquid crystal. Although the formation of a chain structure with a well-defined interparticle distance observed in Refs. [8,13,26] can be attributed purely to the minimization of the elastic energy of nematic liquid crystals, the interparticle distance is determined by the balance between the dipole-dipole attraction and repulsion arising from the

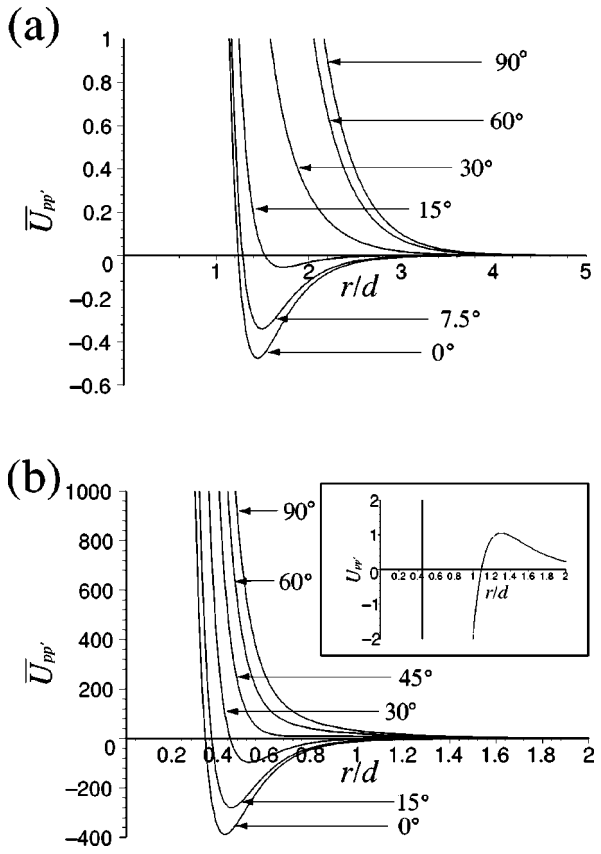

FIG. 2. Reduced pairwise interaction energy $\overline{U}_{pp'} \equiv 4\pi K d^5 U_{pp'}/\Gamma^2$ as a function of reduced particle distance r/d for (a) $r_z^{(p)} = r_z^{(p')} = 0.9d$ and (b) $r_z^{(p)} = r_z^{(p')} = 0.8d$ (region I). The numbers indicate the angle ϕ between $\boldsymbol{r}^{(pp')}$ and the x axis. The inset of (b) is a magnified plot for $\phi = 30°$.

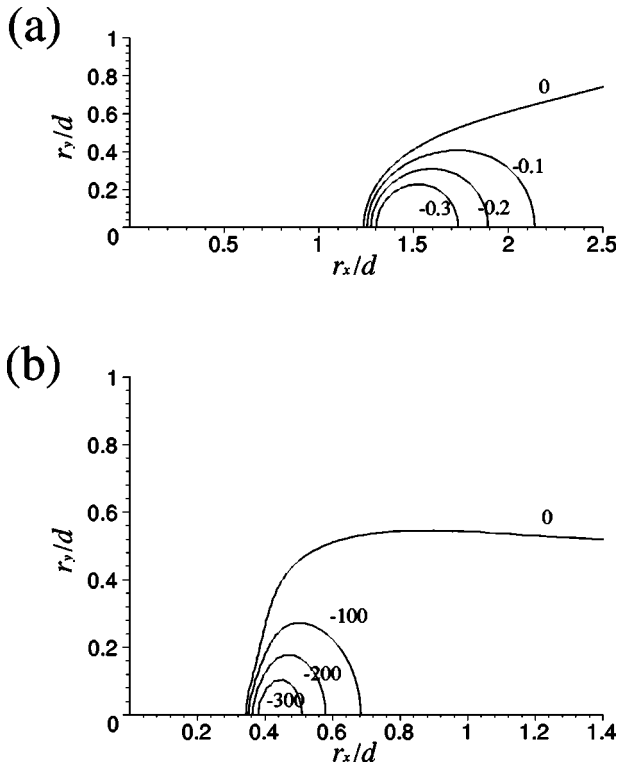

FIG. 3. Contour plots of the reduced interaction energy $\overline{U}_{pp'}$ for (a) $r_z^{(p)} = r_z^{(p')} = 0.9d$ and (b) $r_z^{(p)} = r_z^{(p')} = 0.8d$ corresponding to Fig. 2 (region I). Here r_x and r_y are the abbreviations of $r_x^{(pp')}$ and $r_y^{(pp')}$, respectively. The numbers in the plots are the values of $\overline{U}_{pp'}$. For clarity we have plotted only curves with $\overline{U}_{pp'} \leqslant 0$.

unfavorable elastic deformation due to the presence of topological defects. The situation is therefore different from ours because we deal with the case of weak anchoring and no topological defects. We also point out that in Ref. [28] the formation of a crystal structure by glycerol droplets was attributed to the coexistence of a dipole-dipole attraction and a quadrupole-quadrupole repulsion between droplets. In their interpretation, however, the dipole-dipole interaction can be present only in the case of particles with lower symmetries (they regard the highly distorted region as a particle) and in our case we deal with particles with a spherical symmetry. Therefore we believe that we have presented an example of the possibility of forming a superstructure of particles in a liquid crystal of a completely different origin from previous examples.

We also present the interaction energy for region II with $r_z^{(p)} = r_z^{(p')} = 0.75d$, $0.5d$, and $0.35d$ in Figs. 4 and 5. Note that $\phi_1 = 27.33°$, $61.26°$, and $66.50°$ for $r_z^{(p)} = 0.75d$, $0.5d$, and $0.35d$, respectively. As discussed above, the interaction is repulsive for $\phi > \phi_1$ and attractive for $\phi < \phi_1$ at $r \to 0$. From Fig. 4 we can also observe a potential minimum as in region I for ϕ larger than but close to ϕ_1, and it becomes less evident and eventually vanishes in some cases with larger ϕ. The oscillating behavior of the interaction potential is also present, as can be seen in the insets of Figs. 4(a) and 4(c). The complexity of the interaction landscape is more evident in Fig. 5, which shows that it is sensitively dependent on the z coordinate of the particle position. We also observe from Fig. 5(b) that the interaction can be attractive even at $\phi = 90°$ in the case of $r_z^{(p)} = r_z^{(p')} = 0.5d$, although this attraction is rather weak as can be seen from Fig. 4(b).

Finally, in Figs. 6 and 7 we show the interaction energy of particles in region III, close to the lower confining plates with planar anchoring for $r_z^{(p)} = r_z^{(p')} = 0.32d$ and $0.1d$. We notice that $(\phi_1, \phi_2) = (67.17°, 10.68°)$ and $(69.87°, 29.32°)$ for $r_z^{(p)} = 0.32d$ and $0.1d$, respectively. The interaction at $r \to 0$ is attractive for $\phi_2 < \phi < \phi_1$ and repulsive otherwise as discussed above. From Figs. 6(b) and 6(d) we notice that the behavior of the interaction around ϕ_1 is similar to that in the case of region II. However, it can be seen from Figs. 6(a) and 6(c) the interaction potential close to ϕ_2 sensitively depends on ϕ as well as $r_z^{(p)}$. In the case of $r_z^{(p)} = 0.32d$, the interaction potential has its minimum for all $\phi < \phi_2$ and is a monotonic function for $\phi > \phi_2$. On the other hand, we find that for $r_z^{(p)} = 0.1d$ the interaction potential is repulsive and monotonic for $\phi \lesssim 20°$, and a potential minimum appears at $\phi \simeq 25°$, whose value becomes smaller rapidly with increasing ϕ before reaching ϕ_2. We also observe that at $\phi = 30°$ the interaction possesses a large maximum in contrast to the other cases (notice the difference in the vertical scale from

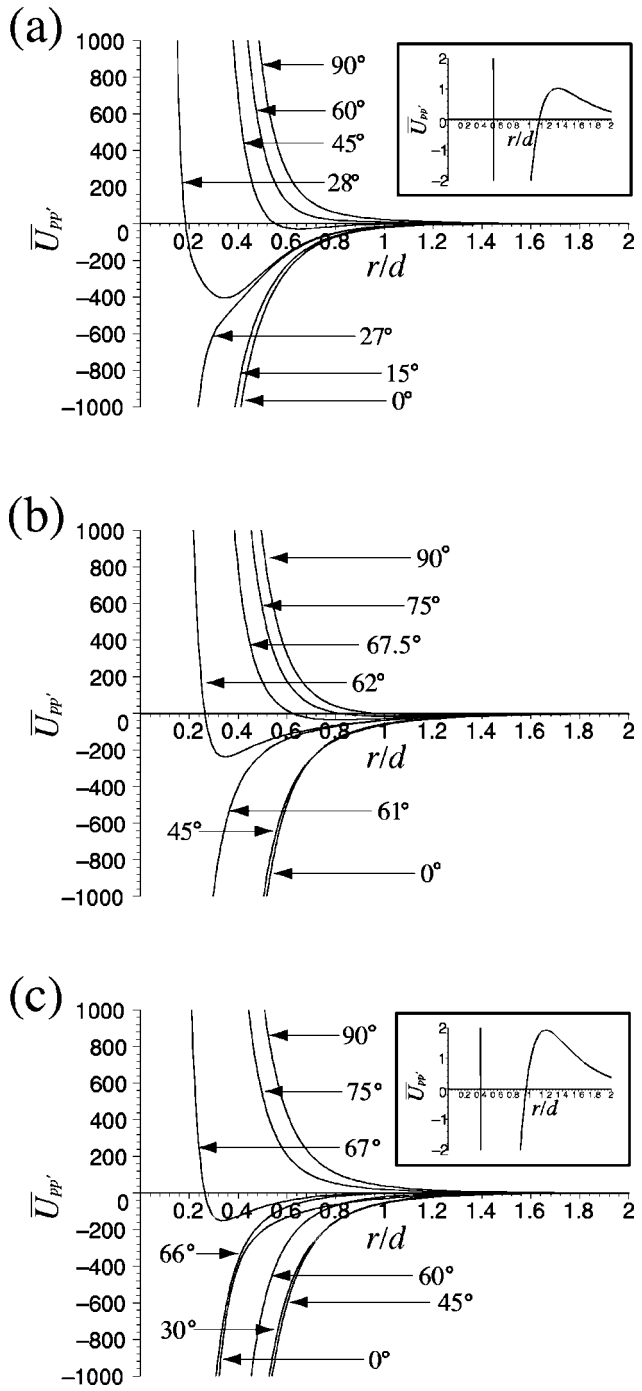

FIG. 4. The same as Fig. 2 for (a) $r_z^{(p)}=r_z^{(p')}=0.75d$, (b) $r_z^{(p)}=r_z^{(p')}=0.5d$, and (c) $r_z^{(p)}=r_z^{(p')}=0.35d$ (region II). The insets are magnified plots for (a) $r_z^{(p)}=r_z^{(p')}=0.75d$, $\phi=45°$ and (c) $r_z^{(p)}=r_z^{(p')}=0.35d$, $\phi=67°$.

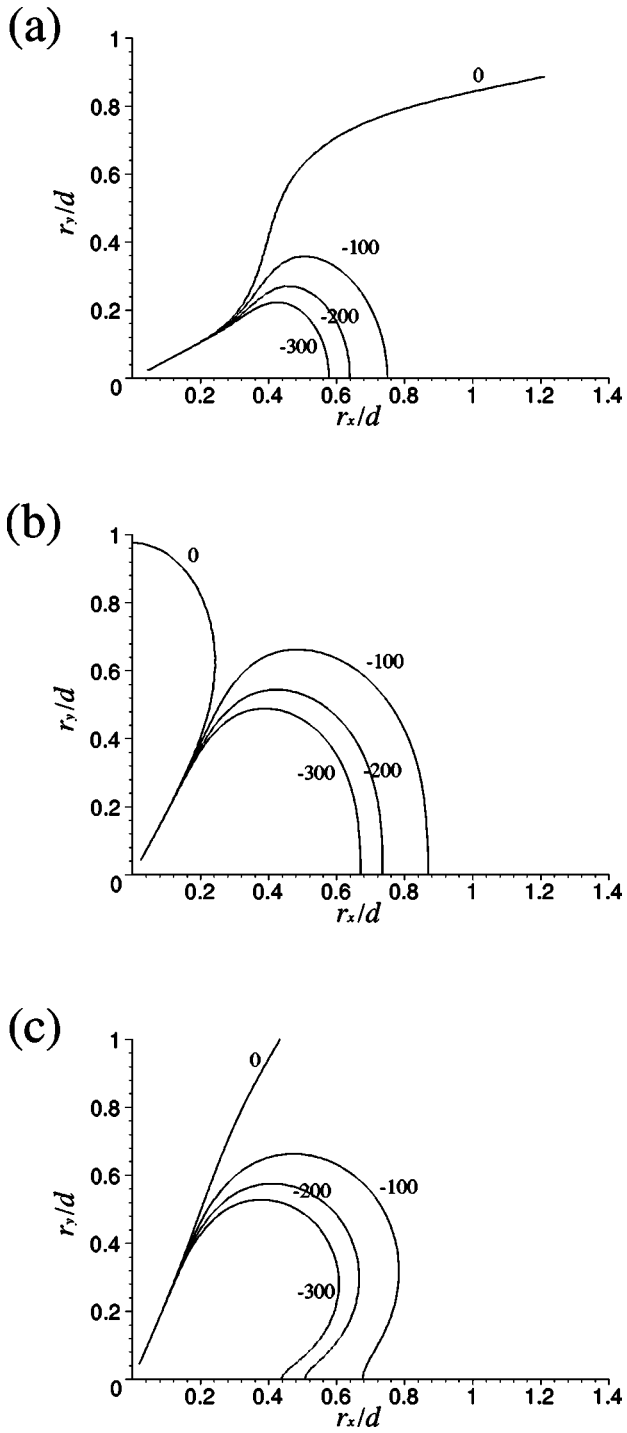

FIG. 5. The same as Fig. 3 for (a) $r_z^{(p)}=r_z^{(p')}=0.75d$, (b) $r_z^{(p)}=r_z^{(p')}=0.5d$, and (c) $r_z^{(p)}=r_z^{(p')}=0.35d$ corresponding to Fig. 4 (region II).

the other graphs). The interaction landscape given in Fig. 7 also shows its complexity and the sensitive dependence on the z coordinate of the particles as in region II. A weak attractive interaction as argued above and found in Fig. 5(b) ($r_z^{(p)}=0.5d$) is also present in region III. However, the direction along which it exists is different according to $r_z^{(p)}$: $\phi=0°$ for $r_z^{(p)}=0.32d$ and $\phi=90°$ for $r_z^{(p)}=0.1d$.

IV. CONCLUDING REMARKS

To investigate the effect of the initial deformation of a liquid crystal on the formation of superstructures of particles immersed in it, we calculated the interaction energy between particles induced by the elastic deformation of a nematic liquid crystal confined in a cell with hybrid boundary conditions, strong homeotropic anchoring on the surface of one

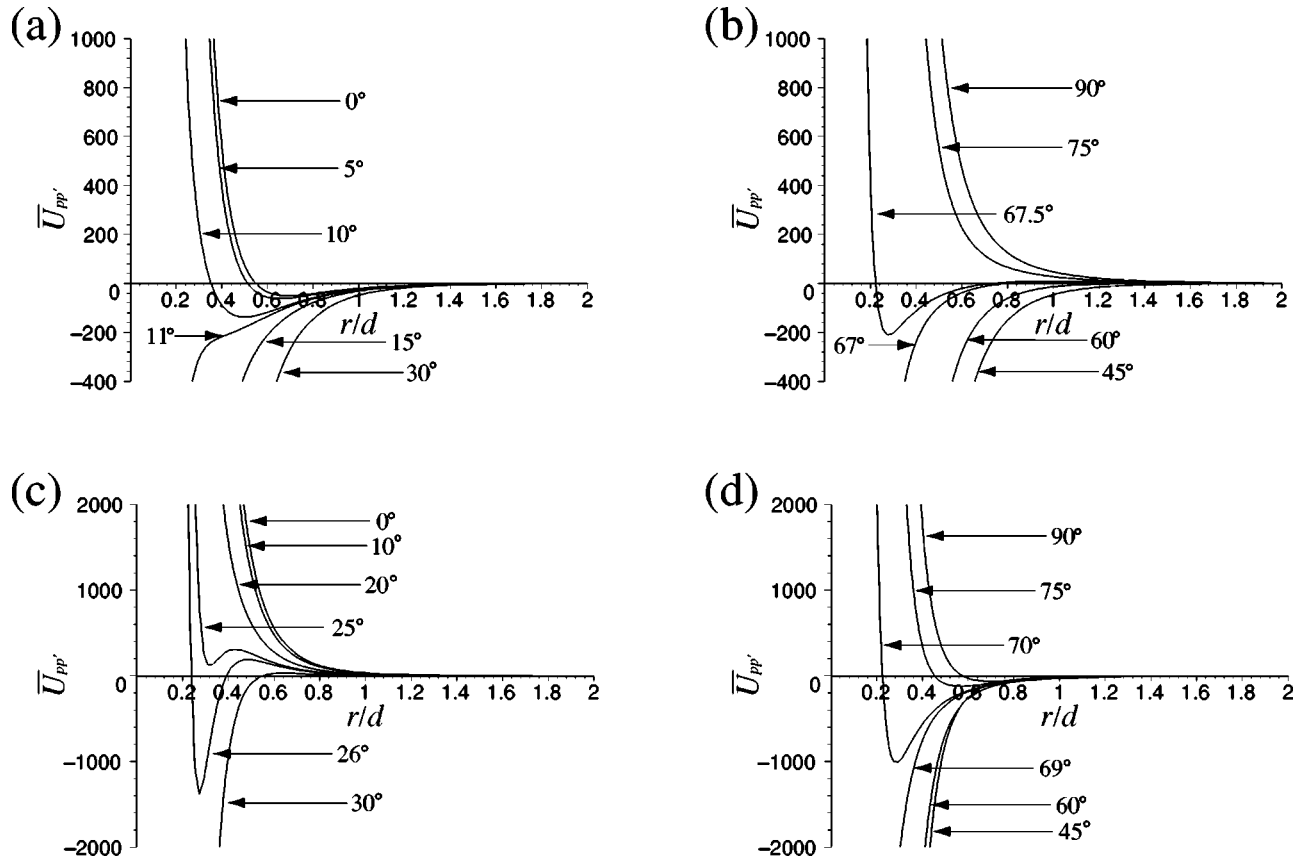

FIG. 6. The same as Figs. 2 and 4 for (a),(b) $r_z^{(p)}=r_z^{(p')}=0.32d$ and (c),(d) $r_z^{(p)}=r_z^{(p')}=0.1d$ (region III). The curves have been given separately for the same $r_z^{(p)}$ just for clarity of the presentation.

confining plate, and strong planar anchoring with fixed in-plane orientation on the other. In the case of weak anchoring on the particle surface and the resultant weak elastic deformation of the director field, we obtained an analytic formula [Eq. (28)] for the interaction energy. The interaction energy has a much more complex form than in the case of uniform nematics or smectics in previous theoretical studies, which reflects the presence of the initial deformed structure of a nematic liquid crystal due to the boundary conditions. We showed by numerical evaluation of Eq. (28) that the interaction potential crucially and sensitively depends on how the two particles are placed with respect to the deformed structure of a nematic liquid crystal and shows a rich and nontrivial potential landscape. One of the significant characteristics is that under appropriately chosen conditions the interaction potential can have a minimum, in contrast with those in previous theoretical studies concerning the elasticity-mediated interaction in liquid crystals. This complex interaction might significantly influence the aggregation kinetics as well as the equilibrium structure of colloidal particles.

Recent experiments by Nazarenko *et al.* [28] show the formation of a crystal structure of droplets in a hybrid cell. The density of droplets in the crystalline hexagonal structure they observe is quite high. Our results anticipate such a hexagonal structure only when the particles are confined to give high density near the upper homeotropic boundary in region I. As shown in Fig. 2(a), the interaction sensitively depends on ϕ, the angle between the distance $\boldsymbol{r}^{(pp')}$ and the direction of the planar anchoring on the lower boundary, at distances larger than the cell spacing d. The interaction is purely repulsive for shorter distances. So if the particles are confined at high density, the particles should form slightly deformed hexagonal ordering due to repulsive interaction. When the density is low, we anticipate the formation of a chainlike superstructure in the same region (close to the upper homeotropic boundary), due to the interaction with the potential minimum at $\phi=0$, which is parallel to the direction of planar anchoring at the lower boundary.

We also point out several causes that can make the experimental results [28] different from our calculation. One is that in the experiments the in-plane orientation on the lower boundary is not fixed and depends on the preparation of the experimental system. A similar calculation with this tangential boundary condition imposed on the lower plate is possible and a qualitatively different result is expected because in that case the rotation associated with v in Eq. (3) becomes a Goldstone mode. However, in the course of the calculation we will suffer from an infrared divergence associated with this Goldstone mode and a careful treatment will be necessary. One cannot rule out another possibility: that the in-plane orientation on the lower boundary is not uniform, in which case analytical treatment will of course be far more difficult. Another possible reason for the difference from the

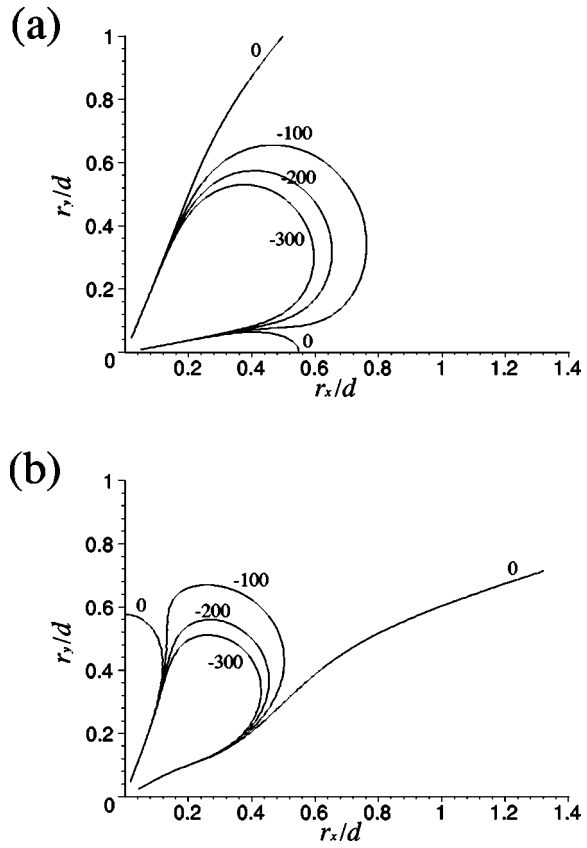

FIG. 7. The same as Figs. 3 and 5 for (a) $r_z^{(p)}=r_z^{(p')}=0.32d$ and (b) $r_z^{(p)}=r_z^{(p')}=0.1d$ corresponding to Fig. 6 (region III).

experimental results is that as noted in Ref. [28] the particle may not be treated as a sphere. Although the weak anchoring condition is satisfied in the experiment of Nazarenko *et al.* [28,44], for a relatively large droplet there might be a case where $|W|r_0/K\sim 1$ and our analyses cannot be justified. In such a case we have to deal with the particle as ''coated'' by the region with strong director deformation [38]. The ''coat'' will be deformed according to the initial director deformation of the nematic liquid crystal and the operators $\mathcal{D}_{1,2}^{(p)}$ in Eq. (28) will have a more complicated form than in our treatment for spherical particles presented in this paper.

In conclusion, we believe that we have proposed a different possibility of forming a superstructure of particles by deforming the liquid crystal in which the particles are immersed. Moreover, we have pointed out the possibility of the formation of a chain structure which might be observable in an experiment with carefully prepared boundary conditions and a low particle density. The energy of a deformed liquid crystal is higher than that of its ground state and the incorporation of foreign particles can relax the excess energy due to the imposed deformation, thus leading to the possibility of a richer variety of behaviors of foreign particles than in the case of an undeformed liquid crystal. To our knowledge, no attention has been paid so far to the effect of the deformation of a liquid crystal on the formation of superstructures of foreign particles, and we hope that experimental and theoretical studies in this direction will be promoted.

ACKNOWLEDGMENTS

We would like to thank Dr. Jun Yamamoto and Dr. Masamitsu Ishitobi for helpful discussions and comments.

APPENDIX: EVALUATION OF $U_{pp'}$

By noticing the identity

$$\frac{1}{(2\pi)^2}\int d^2\boldsymbol{q}_\perp \frac{e^{i\boldsymbol{q}_\perp\cdot\boldsymbol{r}_\perp}}{\boldsymbol{q}_\perp^2+a^2}=\frac{1}{2\pi}K_0(a|\boldsymbol{r}_\perp|), \tag{A1}$$

with a being a positive number and K_0 the modified Bessel function of zeroth order, we can rewrite the interaction energy (27) as

$$\begin{aligned} U_{pp'}(\boldsymbol{r}^{(p)},\boldsymbol{r}^{(p')}) &= -\frac{1}{2\pi Kd}\{\mathcal{D}_1^{(p)}\mathcal{D}_1^{(p')}[\tilde{h}_1(|\boldsymbol{r}_\perp^{(pp')}|,r_z^{(p)}-r_z^{(p')}) \\ &\quad -\tilde{h}_1(|\boldsymbol{r}_\perp^{(pp')}|,r_z^{(p)}+r_z^{(p')})] \\ &\quad +\mathcal{D}_2^{(p)}\mathcal{D}_2^{(p')}[\tilde{h}_2(|\boldsymbol{r}_\perp^{(pp')}|,r_z^{(p)}-r_z^{(p')}) \\ &\quad -\tilde{h}_2(|\boldsymbol{r}_\perp^{(pp')}|,r_z^{(p)}+r_z^{(p')})]\}, \end{aligned} \tag{A2}$$

where $\boldsymbol{r}_\perp^{(pp')}=\boldsymbol{r}_\perp^{(p)}-\boldsymbol{r}_\perp^{(p')}$ and we have defined

$$\tilde{h}_1(\xi,\eta)=\sum_{m=1}^{\infty}K_0(2mq_0\xi)\cos(2mq_0\eta), \tag{A3}$$

$$\tilde{h}_2(\xi,\eta)=\sum_{m=1}^{\infty}K_0\left(2\sqrt{m^2-\frac{1}{4}}q_0\xi\right)\cos(2mq_0\eta). \tag{A4}$$

Using the formula found in Ref. [45], we obtain

$$\begin{aligned} \tilde{h}_1(\xi,\eta) &= \frac{1}{2}\left(\gamma+\ln\frac{q_0\xi}{2\pi}\right)+\frac{\pi}{4q_0}\frac{1}{\sqrt{\xi^2+\eta^2}} \\ &\quad +\frac{\pi}{4q_0}\sum_{m=1}^{\infty}\left\{\frac{1}{\sqrt{\xi^2+(\eta-m\pi/q_0)^2}}\right. \\ &\quad \left.+\frac{1}{\sqrt{\xi^2+(\eta+m\pi/q_0)^2}}-\frac{2q_0}{m\pi}\right\}, \end{aligned} \tag{A5}$$

where γ is Euler's constant.

To evaluate Eq. (A4), we make use of the formula [46]

$$\int_0^\infty d\zeta\frac{\cos(p\sqrt{\zeta^2+X^2})}{\sqrt{\zeta^2+X^2}}\cos(m\zeta)=K_0(\sqrt{m^2-p^2}X), \tag{A6}$$

which holds for $X>0$ and $m>p>0$. By setting $p=1/2$, we have

$$\sum_{m=1}^{\infty} K_0\left(\sqrt{m^2-\frac{1}{4}}X\right)\cos(mY) = \int_0^{\infty} d\zeta \frac{\cos\left(\frac{1}{2}\sqrt{\zeta^2+X^2}\right)}{\sqrt{\zeta^2+X^2}} \sum_{m=1}^{\infty} \cos(m\zeta)\cos(mY). \tag{A7}$$

Noticing the identity

$$\sum_{m=1}^{\infty} \cos(m\zeta)\cos(mY) = -\frac{1}{2} + \frac{\pi}{2} \sum_{m=-\infty}^{\infty} [\,\delta(\zeta+Y-2m\pi) + \delta(\zeta-Y-2m\pi)], \tag{A8}$$

and taking care of the inequality $\zeta \geqslant 0$, we obtain, by setting $X=2q_0\xi$ and $Y=2q_0\eta$, that

$$\tilde{h}_2(\xi,\eta) = \frac{\pi}{4}N_0(q_0\xi) + \frac{\pi}{4q_0}\frac{\cos(q_0\sqrt{\xi^2+\eta^2})}{\sqrt{\xi^2+\eta^2}} + \frac{\pi}{4q_0}\sum_{m=1}^{\infty}\left\{\frac{\cos[q_0\sqrt{\xi^2+(\eta-m\pi/q_0)^2}]}{\sqrt{\xi^2+(\eta-m\pi/q_0)^2}} + \frac{\cos[q_0\sqrt{\xi^2+(\eta+m\pi/q_0)^2}]}{\sqrt{\xi^2+(\eta+m\pi/q_0)^2}}\right\}, \tag{A9}$$

where N_0 is the Neumann function of zeroth order. We arrive at Eq. (28) by using Eqs. (A2), (A5), (A9), and (2).

We note that $\tilde{h}_1(\xi,\eta)$ and $\tilde{h}_2(\xi,\eta)$ become singular at $\xi \to 0$. For finite η, however, this singularity is attributed to the first term of Eqs. (A5) and (A9), which exactly vanishes in the evaluation of Eq. (A2). Therefore the resultant form (28) is well defined even in the case of $|\boldsymbol{r}_{\perp}^{(pp')}|=0$ as long as $\boldsymbol{r}^{(p)} \neq \boldsymbol{r}^{(p')}$.

[1] W.B. Russel, D.A. Saville, and W.R. Schowalter, *Colloidal Dispersions* (Cambridge University Press, Cambridge, England, 1995).

[2] A.P. Gast and C.F. Zukoski, Adv. Colloid Interface Sci. **30**, 153 (1989).

[3] J.N. Israelachvili, *Intermolecular and Surface Forces* (Academic Press, London, 1992).

[4] V.M. Mostepanenko and N.N. Trunov, *The Casimir Effect and Its Application* (Clarendon Press, Oxford, 1997).

[5] A. Borštnik, H. Stark, and S. Žumer, Phys. Rev. E **60**, 4210 (1999).

[6] P. Galatola and J.-B. Fournier, Phys. Rev. Lett. **86**, 3915 (2001).

[7] P. Poulin, V.A. Raghunathan, P. Richetti, and D. Roux, J. Phys. II **4**, 1557 (1994); V.A. Raghunathan, P. Richetti, and D. Roux, Langmuir **12**, 3789 (1996); V.A. Raghunathan, P. Richetti, D. Roux, F. Nallet, and A.K. Sood, Mol. Cryst. Liq. Cryst. Sci. Technol., Sect. A **288**, 181 (1996); Langmuir **16**, 4720 (2000).

[8] P. Poulin, H. Stark, T.C. Lubensky, and D.A. Weitz, Science **275**, 1770 (1997).

[9] P. Poulin, Curr. Opin. Colloid Interface Sci. **4**, 66 (1999).

[10] M. Zapotocky, L. Ramos, P. Poulin, T.C. Lubensky, and D.A. Weitz, Science **283**, 209 (1999).

[11] S.P. Meeker, W.C.K. Poon, J. Crain, and E.M. Terentjev, Phys. Rev. E **61**, R6083 (2000).

[12] J. Yamamoto and H. Tanaka, Nature (London) **409**, 321 (2001).

[13] P. Poulin and D.A. Weitz, Phys. Rev. E **57**, 626 (1998).

[14] O. Mondain-Monval, J.C. Dedieu, T. Gulik-Krzywicki, and P. Poulin, Eur. Phys. J. B **12**, 167 (1999).

[15] Y. Gu and N.L. Abbott, Phys. Rev. Lett. **85**, 4719 (2000).

[16] E.M. Terentjev, Phys. Rev. E **51**, 1330 (1995).

[17] O.V. Kuksenok, R.W. Ruhwandl, S.V. Shiyanovskii, and E.M. Terentjev, Phys. Rev. E **54**, 5198 (1996).

[18] T.C. Lubensky, D. Pettey, N. Currier, and H. Stark, Phys. Rev. E **57**, 610 (1998).

[19] S.V. Shiyanovskii and O.V. Kuksenok, Mol. Cryst. Liq. Cryst. Sci. Technol., Sect. A **321**, 45 (1998).

[20] R.W. Ruhwandl and E.M. Terentjev, Phys. Rev. E **56**, 5561 (1997).

[21] H. Stark, Eur. Phys. J. B **10**, 311 (1999); Phys. Rep. **351**, 387 (2001).

[22] J.L. Billeter and R.A. Pelcovits, Phys. Rev. E **62**, 711 (2000).

[23] D. Andrienko, G. Germano, and M.P. Allen, Phys. Rev. E **63**, 041701 (2001).

[24] J. Fukuda and H. Yokoyama, Eur. Phys. J. E **4**, 389 (2001); J. Fukuda, M. Yoneya, and H. Yokoyama, Phys. Rev. E **65**, 041709 (2002).

[25] P. Poulin, V. Cabuil, and D.A. Weitz, Phys. Rev. Lett. **79**, 4862 (1997).

[26] J.-C. Loudet, P. Barois, and P. Poulin, Nature (London) **407**, 611 (2000).

[27] P. Poulin, N. Francès, and O. Mondain-Monval, Phys. Rev. E **59**, 4384 (1999).

[28] V.G. Nazarenko, A.B. Nych, and B.I. Lev, Phys. Rev. Lett. **87**, 075504 (2001).

[29] S.L. Lopatnikov and V.A. Namiot, Zh. Éksp. Teor. Fiz. **25**, 361 (1978) [Sov. Phys. JETP **48**, 180 (1978)].

[30] S. Ramaswamy, R. Nityananda, V.A. Raghunathan, and J. Prost, Mol. Cryst. Liq. Cryst. Sci. Technol., Sect. A **288**, 175 (1996).

[31] R.W. Ruhwandl and E.M. Terentjev, Phys. Rev. E **55**, 2958 (1997).

[32] H. Stark, J. Stelzer, and R. Bernhard, Eur. Phys. J. B **10**, 515 (1999).

[33] M.S. Turner and P. Sens, Phys. Rev. E **55**, R1275 (1997); P. Sens, M.S. Turner, and P. Pincus, *ibid.* **55**, 4394 (1997); P. Sens and M.S. Turner, J. Phys. II **7**, 1855 (1997); M.S. Turner and P. Sens, Phys. Rev. E **57**, 823 (1998).

[34] J. Groenwold and G.H. Fredrickson, Eur. Phys. J. E **5**, 171 (2001).

[35] K.M. Aoki, B.I. Lev, and H. Yokoyama, Mol. Cryst. Liq.

Cryst. Sci. Technol., Sect. A **367**, 537 (2001); B.I. Lev, K.M. Aoki, P.M. Tomchuk, and H. Yokoyama (unpublished).
[36] R. Yamamoto, Phys. Rev. Lett. **87**, 075502 (2001).
[37] B.I. Lev and P.M. Tomchuk, Phys. Rev. E **59**, 591 (1999).
[38] B.I. Lev, S.B. Chernyshuk, P.M. Tomchuk, and H. Yokoyama, Phys. Rev. E **65**, 021709 (2002).
[39] J. Fukuda, B.I. Lev, and H. Yokoyama, Phys. Rev. E **65**, 031710 (2002).
[40] There is also a recent experiment of photopolymerization-induced phase separation in a deformed liquid crystal by Volcoschenko *et al.* (e-print cond-mat/0109473), which revealed the accumulation of polymer droplets into regions with high elastic energy of liquid crystals. This experimental situation is different from that in this paper because we deal with a system whose elastic energy density in the absence of particles is spatially uniform.
[41] P.G. de Gennes and J. Prost, *The Physics of Liquid Crystals*, 2nd ed. (Oxford University Press, Oxford, 1993).
[42] In this form of the Frank elastic energy we implicitly set the saddle-splay elastic constant as $K_{24}=K$. The possible effect of the saddle-splay elasticity on the equilibrium director configuration in a hybrid nematic cell is discussed by A. Sparavigna, L. Komitov, O.D. Lavrentovich, and A. Strigazzi, J. Phys. II **2**, 1881 (1992).
[43] A. Rapini and M. Papoular, J. Phys. Colloq. **30**, C4-54 (1969).
[44] Since the anchoring energy of a liquid crystal with glycerol is $W\sim10^{-3}$–10^{-4} erg/cm^2 and the Frank elastic constant K is of the order 10^{-6} dyn, the weak anchoring condition $|W|r_0/K \ll 1$ is satisfied for micrometer-size droplets in the experiment of Ref. [28].
[45] I.S. Gradshteyn and I.M. Ryzhik, *Tables of Integrals, Series and Products*, 5th ed. (Academic Press, New York, 1994), p. 992.
[46] I.S. Gradshteyn and I.M. Ryzhik, *Tables of Integrals, Series and Products*, 5th ed. (Ref. [45]), p. 508.